AN EXTENDED SUPERSONIC COMBUSTION MODEL FOR THE DYNAMIC ANALYSIS OF HYPERSONIC VEHICLES

Interim Task Report

for

NASA Grant NAG-1-1341

On Research Performed for the

NASA Langley Research Center

Hampton, VA

Principal Investigators

J.A. Bossard, Dr. R.E. Peck, and Dr. D.K. Schmidt

Aerospace Research Center

College of Engineering and Applied Sciences

Arizona State University
Tempe, AZ 85287-8006

Internal Report No. ARC93-2

March 1993

Table of Contents

Abstract

The development of an advanced dynamic model for aeroelastic hypersonic vehicles powered by air breathing engines requires an adequate engine model. This report provides a discussion of some of the more important features of supersonic combustion and their relevance to the analysis and design of supersonic ramjet engines. Of particular interest are those aspects of combustion that impact the control of the process. Furthermore, the report summarizes efforts to enhance the aeropropulsive/aeroelastic dynamic model developed at the Aerospace Research Center of Arizona State University by focusing on combustion and improved modeling of this flow. The expanded supersonic combustor model described here has the capability to model the effects of friction, area change, and mass addition, in addition to the heat addition process. A comparison is made of the results from four cases: 1) heat addition only, 2) heat addition plus friction, 3) heat addition, friction, and area reduction, and 4) heat addition, friction, area reduction, and mass addition. The relative impact of these effects on the Mach number, static temperature, and static pressure distributions within the combustor are then shown. Finally, the effects of frozen versus equilibrium flow conditions within the exhaust plume is discussed.

Nomenclature

A	Cross sectional Area of Combustor (ft^2)
A_2	Combustor Inlet cross sectional Area (ft^2)
A_3	Combustor Exit cross sectional Area (ft^2)
c_p	specific heat (Btu/lbm $\cdot^oR$)
f	friction coefficient
F_A	Area Change Influence Coefficient; (eqn. 3.1-8b)
F_{T0}	Heat Transfer Influence Coefficient; (eqn. 3.1-8c)
F_f	Friction Influence Coefficient; (eqn. 3.1-8d)
F_w	Mass Addition Influence Coefficient; (eqn. 3.1-8e)
D	Combustor Duct Hydraulic Diameter (ft); ($D = 4A/P_w$)
h	Convection Heat Transfer Coefficient ($Btu/hr \cdot ft^2 \cdot^oR$)
$\dot{m}_f$	Fuel mass flow rate (lbm/sec)
$\dot{m}_{air}$	Air mass flow rate (lbm/sec)
$\overline{M}$	Mean Mach Number
M_2	Combustor Inlet Mach Number
M_3	Combustor Exit Mach Number
P_2	Combustor Inlet Static Pressure (Psf)
P_3	Combustor Exit Static Pressure (Psf)
P_w	Wetted Perimeter of Combustor (ft)
Q	Heating Value of fuel (Btu/lbm)
T_2	Combustor Inlet Static Temperature (^oR)
T_{02}	Combustor Inlet Stagnation Temperature (^oR)
T_{03}	Combustor Exit Stagnation Temperature (^oR)
V	Gas Volume (ft^3)
x	weighting value (eqn. 3.1-9a)
$x_3 - x_2$	Combustor Length (ft)
γ	Ratio of Specific Heats
ρ	Air density (lbm/ft^3)

I. Introduction

Advanced hypersonic vehicles and single-stage-to-orbit spacecraft will require air breathing engines to achieve long cruise ranges and high payload-to-orbit fractions. Yet the formation of an applicable dynamic model for this class of vehicle is a formidable task. Previous work at the Aerospace Research Center of Arizona State University has sought to develop such a dynamical model which integrates the aerodynamics and propulsive effects on a generic hypersonic air breathing vehicle.

Central to the development of such a model is the analysis of the propulsive engine of this vehicle. The dynamical model developed by the Aerospace Research Center assumes that the engine is a Supersonic Combustion Ramjet, i.e. a scramjet. Like the ramjet engine cycle, the scramjet uses aerodynamic shapes to shock-compress the incoming air flow. However, instead of decelerating the flow to subsonic velocities, the flow through the scramjet remains supersonic, only nearing sonic velocity at the combustor exit. Thermal energy is supplied to the airflow from the combustion of fuel at supersonic speeds. In principle, the supersonic combustion process is relatively straightforward. However, little experimental data currently exists for actual supersonic combustors. Furthermore, a complete scramjet-cycle engine has yet to be flight-tested in the U.S.

Efforts at the ARC have sought to develop a cohesive analytic model of the dynamics of such a hypersonic vehicle. References [1] and [2] describe in detail this work. In these reports, the engine module consisted of a diffuser, combustor, and internal nozzle. The assumptions that went into the combustion analysis consisted of a simple, 1-D, Rayleigh-Line heat addition process, followed by a 1-D, isentropic, internal nozzle expansion. The exit of the internal nozzle marks the end of the engine module.

After exiting the internal nozzle, the flow expands in an external nozzle, where the under surface of the airframe acts as one wall of the nozzle, and a free-stream shear

layer acts as the other effective wall. Gas properties in the external nozzle expansion of the combustion gases is evaluated by equating freestream and exhaust plume pressures along the plume/free-stream shear-layer interface.

This report begins with a qualitative description of the supersonic combustion process, outlining the thermodynamic necessity for the supersonic combustion process at hypersonic flight Mach numbers, the time limiting processes in supersonic combustion, and shock/combustion interactions. The report then proceeds to a description of efforts to enhance the engine model by accounting for the additional effects of friction, area change, and mass addition on the combustion process. The current combustion model consists of a simple, one-dimensional gas flow in which heat addition takes place, a type of compressible flow commonly known as Rayleigh Flow. To examine the comparative impact of these additional effects, four different test cases were evaluated: Case 1: heat addition only, as in the original engine model, Case 2: heat addition with friction, Case 3: heat addition, friction, and area reduction, and Case 4: heat addition, friction, area reduction, and mass addition. A comparison of the results from these four cases is presented by showing the Mach number, static temperature, and static pressure distributions which more clearly illustrates the relative impact of these additional processes.

The equations describing the change in the state variables are similar in form to those describing only Rayleigh Flow. The combustion sensitivity coefficients can then be computed in the same manner as that of the previous work [1], thus allowing them to be incorporated into the analytic expressions for the overall engine model, and hopefully improve the dynamic model.

Finally, a discussion of the external nozzle expansion is presented. This section gives details of this expansion process and, most importantly, provides information on the effect of frozen versus equilibrium flow in this nozzle and its impact on overall engine performance.

II. The Supersonic Combustion Process

2.1 Necessity of the Supersonic Combustion Process

At around Mach 6, the stagnation temperature of the air entering a ramjet engine, after being shock-compressed and decelerated to subsonic velocities, becomes so high that any energy addition from combustion is absorbed by the formation of dissociated reaction products, and hence cannot be used to accelerate the air stream to produce thrust. Dissociated products are chemical compounds from the combustion process that, because of extreme thermal agitation, have been ionized and form a mixture of ionized species and electrons.

The supersonic combustion process mitigates this problem by avoiding the deceleration of the air stream to subsonic velocities and instead adds enthalpy while the air steam continues to travel at supersonic speeds. Nevertheless, it comes with its own set of problems, such as very short residence times, shock/combustion interactions, and combustion instabilities.

2.2 Residence Time Limitations

The combustion process can be broken down into three main time-limiting processes: vaporization, mixing, and chemical reactions. The vaporization process applies to the addition of liquid fuels. This report implicitly assumes only the addition of gaseous fuels, thus the vaporization process will not be considered here. In the mixing process, molecules of fuel must become physically adjacent to air molecules in order for a chemical reaction to take place. On a macroscopic scale, this takes place from bulk fluid motions, and is expedited by turbulence, boundary layers, and shock waves in the scramjet engine.

Once the fuel and air molecules are adjacent, the rate at which the chemical reaction can proceed dictates the combustion rate. This is determined by the chemical kinetics of the reactants, and by reactant state properties, such as temperature and pressure.

In the supersonic combustor, the highly turbulent flow, shock waves, and strong boundary-layer interactions all contribute to the production of a vigorous mixing environment. Thus, it is probably reasonable to assume that the mixing time is short relative to the chemical reaction rate, and that the chemical kinetics are the rate-limiting reaction in the overall combustion process.

In order for the flame to be stabilized within the combustor, the flame speed must always exceed the local flow velocity, otherwise the flame front is swept downstream and the flame is blown out. The flame speed is highly concentration dependent, and therefore is a function of the local fuel-to-air mixture ratio. Flame speeds which exceed the speed of sound are called detonations, subsonic flame speeds are known as deflagrations. Figure 1 shows the detonation flame speed for gaseous hydrogen in air as a function of mixture ratio, by volume [5]. This chart assumes the hydrogen and air are thoroughly mixed prior to combustion. The upper and lower ends of this curve denote the rich and lean mixture ratio limits, respectively, of the hydrogen-air combustion process. Flames cannot be sustained outside of these limits because of an insufficient amount of air at the rich limit, or hydrogen at the lean limit. For the scramjet engine, these limitations constrain the speed at which air can pass through the combustor. Speeds through the combustor above the rich limit will blow out the combustor flame, speeds below the lean limit require excess fuel to be dumped into the combustor, lowering engine performance.

2.3 Shock/Combustion Interactions

Unique to the supersonic combustor is the presence of internal shock waves, both normal and oblique. Shock waves themselves are essentially thermodynamic discontinuities, being of negligible thickness and non-equilibrium processes. Furthermore, shock waves can interact strongly with the boundary layer, producing flow disturbances and boundary layer separation. This situation is exacerbated at the fuel injection sites within the scramjet combustor. Fuel injection from the sidewall of

the combustor produces a local oblique shock which can separate the boundary layer upstream of the injection site. For this reason, it is generally regarded as necessary to have at the fuel injection site an "isolator duct" which serves to isolate flow disturbances caused by the fuel addition process [6]. This translates into the requirement for a slightly longer overall combustor length. Figure 2 illustrates this consideration.

The exact nature of the supersonic air stream's overall interaction with the fuel injection process is currently not well understood. Although most of the important pieces of the injection problem can be described analytically, the ensemble must still be tested experimentally, and much of the current work on scramjet engines is simply to identify geometric features for scramjet fuel injectors that minimize the amount of disturbance to the air stream. Figure 3 shows some of the current thinking for supersonic flame holders [6]. These dimensions give a rough idea of the proportions necessary for an efficient fuel injection geometry.

III. Scramjet Engine Modeling

3.1 Combustor Flow Modeling

In the previous report [1], the modeling of the scramjet engine combustor consisted of performing a simple, 1-D, Rayleigh line analysis in which frictionless heat addition causes a change in stagnation temperature. The energy balance gives us:

$$Q = c_p (T_{03} - T_{02}) \tag{3.1-1}$$

Since

$$T_{03} = T_{02} + \Delta T_0$$

$$\Delta T_0 = \frac{Q}{c_p} \tag{3.1-2}$$

And

$$\frac{T_{03}}{T_{02}} = 1 + \frac{\Delta T_0}{T_{02}}$$

$$= 1 + \frac{\Delta T_0}{T_2}\left(\frac{T_2}{T_{02}}\right) \tag{3.1-3}$$

Also

$$\frac{T_{03}}{T_{02}} = \left(\frac{1+\gamma M_2^2}{1+\gamma M_3^2}\right)\left(\frac{M_3}{M_2}\right)^2 \left[\frac{1+\frac{\gamma-1}{2}M_3^2}{1+\frac{\gamma-1}{2}M_2^2}\right] \tag{3.1-4a}$$

$$\frac{T_2}{T_{02}} = \left[1+\frac{\gamma-1}{2}M_2^2\right]^{-1} \tag{3.1-4b}$$

Substituting and Rearranging:

$$\frac{M_3^2\left(1+\frac{\gamma-1}{2}M_3^2\right)}{\left(\gamma M_3^2+1\right)^2} = \frac{M_2^2\left(1+\frac{\gamma-1}{2}M_2^2\right)}{\left(\gamma M_2^2+1\right)^2} + \frac{M_2^2}{\left(\gamma M_2^2+1\right)^2}\frac{\Delta T_0}{T_2} \tag{3.1-5}$$

The integral relations for gas dynamical flows gives us:

$$P_3 = P_2 \left[\frac{1 + \gamma M_2^2}{1 + \gamma M_3^2} \right] \tag{3.1-6}$$

$$T_3 = T_2 \left\{ \left[\frac{1 + \gamma M_2^2}{1 + \gamma M_3^2} \right] \left(\frac{M_3}{M_2} \right) \right\}^2 \tag{3.1-7}$$

As in the previous report [1].

However, the more general differential form of the momentum equation, accounting for heat transfer, friction, area change, and mass addition is:

$$dM^2 = F_A \frac{dA}{A} + F_{T_0} \frac{dT_0}{T_0} + F_f 4f \frac{dx}{D} + F_w \frac{dw}{w} \tag{3.1-8a}$$

where

$$F_A \equiv - \frac{2M^2 \left(1 + \frac{\gamma - 1}{2} M^2 \right)}{1 - M^2} \tag{3.1-8b}$$

$$F_{T_0} \equiv \frac{M^2 \left(1 + \gamma M^2 \right) \left(1 + \frac{\gamma - 1}{2} M^2 \right)}{1 - M^2} \tag{3.1-8c}$$

$$F_f \equiv \frac{\gamma M^4 \left(1 + \frac{\gamma - 1}{2} M^2 \right)}{1 - M^2} \tag{3.1-8d}$$

$$F_w \equiv \frac{2M^2 \left(1 + \gamma M^2 \right) \left(1 + \frac{\gamma - 1}{2} M^2 \right)}{1 - M^2} \tag{3.1-8e}$$

Under conditions of no friction, area change, or mass addition, then f = 0, dA = 0, and dw = 0, and equation 3.1-8a can be integrated to obtain equation 3.1-5. However, for cases in which any of these terms are non-zero, then equation 3.1-8a cannot be solved in

closed form but must be integrated numerically. The development of this set of equations is detailed in Shapiro [3]. This reference consists of two volumes, and is a recommended source for further reading on the subjects of both theoretical and experimental compressible flows.

Solutions to this set of equations form the basis of the analysis detailed in this report. To solve this set of equations, they were first discretized in an adjustable implicit form, where $\overline{M}$ is a weighted average of M_1 and M_2:

$$\overline{M} = x M_1 + (1 - x) M_2 \tag{3.1-9a}$$

The influence coefficients, corresponding to equations 3.1-8b-e, thus become:

$$\overline{F_A} = -\frac{2\overline{M}^2\left(1 + \frac{\gamma - 1}{2}\overline{M}^2\right)}{1 - \overline{M}^2} \tag{3.1-9b}$$

$$\overline{F_{T_o}} = \frac{\overline{M}^2\left(1 + \gamma\overline{M}^2\right)\left(1 + \frac{\gamma - 1}{2}\overline{M}^2\right)}{1 - \overline{M}^2} \tag{3.1-9c}$$

$$\overline{F_f} = \frac{\gamma\overline{M}^4\left(1 + \frac{\gamma - 1}{2}\overline{M}^2\right)}{1 - \overline{M}^2} \tag{3.1-7d}$$

$$\overline{F_w} = \frac{2M^2\left(1 + \gamma M^2\right)\left(1 + \frac{\gamma - 1}{2}M^2\right)}{1 - M^2} \tag{3.1-9e}$$

Similarly, equation 3.1-8a becomes discretized as:

$$M_2^2 - M_1^2 = \overline{F_{T_o}}\left(\frac{T_{02} - T_{01}}{T_{02}}\right) + \overline{F_f}\left(\frac{4f(x_2 - x_1)}{D}\right) + \overline{F_A}\left(\frac{A_2 - A_1}{A_2}\right) + \overline{F_w}\left(\frac{w_2 - w_1}{w_2}\right) \tag{3.1-9f}$$

These equations could then be coded as a computer program wherein M_2 would be solved for, marching down the combustor length in a step-wise fashion. Selecting a value for x (in equation 3.1-9a) between zero and one allows the user to adjust the numerical sensitivity for each step, as it was found that the system of equations became increasingly ill-conditioned as the value of M_2 approached unity. Typically, x was set at a value of 0.1.

Analogous to the previous work, the local static temperature and pressure are given by integral relations similar to equations 3.1-6 and 3.1-7, but also accounting for the friction, area change, and mass additions effects:

$$P_3 = P_2\left[\frac{1+\gamma M_2^2}{1+\gamma M_3^2}\right]\left(\frac{w_2}{w_1}\right)\left(\frac{A_1}{A_2}\right) \qquad (3.1\text{-}10)$$

$$T_3 = T_2\left\{\left[\frac{1+\gamma M_2^2}{1+\gamma M_3^2}\right]\left(\frac{M_3}{M_2}\right)\right\}^2 \qquad (3.1\text{-}11)$$

The temperature change (i.e. heat addition), area change, and friction distributions were specified over the length of the combustor, and thus were independent variables in the computation. To more closely simulate an actual combustion process, the mass addition distribution was made a function of the heat addition distribution, as can be seen from the more complete energy equation, analogous to equation 3.1-1:

$$\dot{m}_f Q = (\dot{m}_f + \dot{m}_{air})\, c_p\, (T_{03} - T_{02}) \qquad (3.1\text{-}12)$$

where the given ΔT determines the amount of fuel of a specified heating value, Q, that must be added to produce such a temperature rise.

Lastly, the appropriate pieces of this numerical model can be used in the corresponding relationships developed in ref. [1], and the combustion sensitivity coefficients computed in a like manner.

3.2 Combustor Flow Analysis

The scramjet engine geometry assumed in this analysis is shown in figure 4. Station 1 represents the inlet to the engine. Between stations 1 and 2, the diffuser of the engine, the flow is isentropically decelerated. It is assumed that the area ratio between station 1 and 2 can be varied and is a control effector within the dynamics model. Between stations 2 and 3, heat is added by the combustion of fuel (hydrogen) and air. At the end of the combustor, station 3, the Rayleigh-line heat addition process has significantly raised the stagnation temperature, and the flow nears its Rayleigh-line supersonic choking condition, i.e. the local Mach number at station 3 is equal to or just slightly greater than unity. The flow then leaves the combustor and enters a short internal nozzle between stations 3 and e, the engine module exit.

Supersonic combustion occurs between stations 2 and 3. It is within this section that the effects of heat addition, friction, area change, and mass addition may be accounted for, and for which the results presented here are pertinent to. Inlet values used for the combustor were the same used in ref. [1]. These values were:

$T_2 = 2620.38\ ^oR \qquad M_2 = 2.3643 \qquad P_2 = 29779.16\ Psf \qquad \Delta T_o = 2000.0\ ^oR$

To account for the other independent variables (i.e. friction, area change, and mass addition) in the computation, suitable values were selected. For the friction values:

$$f\frac{dx}{D} = (0.0003)(.1) = 0.00003$$

This value for f is representative of a smooth metal surface that has been heavily oxidized, as by combustion. For the area change distribution:

$$A_3 = (0.9)\,A_2$$

Thus, the inlet area is 'closed down' by 10 % over the length of the combustor. It should be mentioned that the area could also be 'opened up' in which case $A_3 > A_2$, but this case was not explored in this study.

Although the mass addition is a function of the heat addition, the heating value of the fuel must be specified. Thus for:

$$Q = 50{,}000 \frac{Btu}{lbm} \quad \text{and} \quad c_p = (.24) \frac{Btu}{lbm \cdot {}^\circ R}$$

which are the heating properties of hydrogen combusted in air, the resulting mass addition to achieve the specified stagnation temperature rise, $\Delta T = 2000$ °R for this study, would require that:

$$w_3 = (1.0096)\, w_2$$

Having specified the independent variables, the Mach number can then be calculated at each step, as detailed in section 3.1. Knowing the local Mach number, the static temperature and pressure can then also be calculated, as per equations 3.1-10,11.

Four cases were prepared to examine the relative impact from each of the four effects modeled. Case 1 represents heat addition only such as was modeled in the original engine analysis from ref. [1]. This case serves as the baseline case. Case 2 includes the effect of friction with heat addition. Case 3 represents heat addition, friction, and area reduction. Case 4 includes all four effects: heat addition, friction, area reduction, and mass addition. Although other combinations of these effects could have been selected, cases 1 and 4 represent essentially the maximum 'bandwidth' for the effects considered here

In figure 5, the Mach number distribution in the scramjet combustor for the four cases is shown. Clearly, the addition of friction, decreasing area, and mass addition all cause the Mach number to decrease more rapidly relative to case 1. Of note is the fact that the effect of area reduction seems to produce the largest relative change. This is probably because the amount of area change selected in these calculations represented the largest relative change among the effects investigated here. Also, the effect of friction is seen to have the least relative impact on the combustion process, judging by how close case 2 lies to case 1.

The local static temperature rise in the combustor is shown in figure 6, again for the four cases. This figure illustrates that the addition of friction, area, and mass to the combustor increases the resulting static temperature, in keeping with the entropic nature of these processes. These results are also consistent with the integral relation between static and stagnation temperature:

$$T_{02} = T_2\left(1 + \frac{(\gamma-1)}{2}M^2\right) \qquad (3.2\text{-}1)$$

Since the stagnation temperature at each step is equal for all four cases, then the reduction in Mach number, as shown in figure 5, means that there must be a corresponding increase in static temperature. Because the static temperature is limited by the allowable material temperature limits of the combustor, the amount of energy that can be added to the combustor is constrained, and the additional effects of friction, area reduction, and mass addition are effectively reductions in the overall efficiency of the supersonic combustion process.

The static pressure rise is shown in figure 7. The addition of friction, reduction in area, and mass all cause the static pressure to increase more rapidly than that of the heat-addition-only case.

In general, the importance of heat addition, friction, area change, and mass addition will be dependent upon the relative size of each of their respective terms in equation 3.1-6. If these terms are of similar order of magnitude, then their effects can be of similar importance. In the analysis performed here, the amount of heat addition is large compared to the other effects, indicating that heat addition effects will dominate this gas dynamical situation.

The inclusion of friction, area change and mass addition in the combustor section of this engine model gives a more complete estimate of engine performance, and allows the validity of the original frictionless, constant area, and no mass addition assumptions to be ascertained. It was shown that the inclusion of the friction, area reduction, and mass addition effects in the combustor decreased the amount of heat that could

effectively be added to the supersonic air stream before reaching the material temperature limits of the combustor walls.

Lastly, the processes investigated here do affect the ability of the scramjet engine to produce thrust, which is its primary function. Relative to the heat addition-only case, the added friction (as in case 2) reduces the thrust by about 4 %, while area reduction reduces it by an additional 8 %, and mass addition an additional 4 %. Thus, the cumulative reduction in thrust from all of these effects would be about 16 %.

IV. External Nozzle Expansion

Yet another unique feature of the currently configured NASP-type vehicle is the use of an external nozzle at the rear of the craft, a "boat-tail" if you will. By using an external expansion process, a large nozzle expansion ratio can be achieved at a relatively small weight penalty. While the engine exit gases expand against the underside of the boat-tail, the free-stream side of the expansion process forms a free-jet boundary, defined by the equilibration of the static pressure of the exhaust plume with the freestream static pressure.

Because of the very high temperatures of the exhaust gas, the combustion products tend to be chemically dissociated, i.e. the reaction products broken up into ionized monatomic and diatomic species. A considerable amount of energy can be tied up in these dissociated states, with the recombination process acting as an effective heat source in the nozzle. However, if there is insufficient time for the dissociated species to recombine during the expansion process, then this energy is lost. In the limit, the expansion process becomes so much faster than the recombination process that no recombination occurs at all, and the nozzle flow is said to be frozen. Energy locked up in dissociated reaction species is thus "thrown away" with the exhaust gases. The frozen condition is an undesirable situation since it represents a loss to overall engine performance.

In figure 8, the specific impulse from a H2-O2 rocket engine is shown as a function of mixture ratio [7]. The experimental results are bracketed by the performance limits of a perfect, equilibrium expansion, and a completely frozen expansion. The chemical kinetics of the H2-O2 combustion process are quite rapid, which partially explains why the experimental results more closely match the equilibrium condition. Fuels with slower chemical kinetics, such as RP-1, have performances more closely matching the frozen flow conditions. Since performance is at a premium, this suggests that scramjet engines may be constrained to use fuels with fast chemical kinetics, such as

hydrogen. These results show that the H2-O2 combustion process comes in closer to an equilibrium performance, and they are also probably adequate to describe the recombination process in the external nozzle expansion of the NASP vehicle if hydrogen is used as the fuel.

V. Summary and Conclusions

As discussed in section II, it becomes clear that the supersonic combustion process is a more complex flow than subsonic combustion, and is less well understood. However, supersonic combustion provides some distinct advantages for air breathing propulsion at higher flight Mach numbers, and in fact becomes a necessity for the flight speeds envisioned for NASP-type vehicles.

As shown in sections 3.1 and 3.2, a more detailed analysis of the combustor section of a scramjet engine model has been undertaken to include the effects of friction, area change, and mass addition in the heat addition process, whereas in the previous model these effects was neglected. Results from the analysis were presented, helping to quantify the effect of friction, area change, and mass addition on combustor performance. These effects, taken together, effectively reduce the amount of thrust produced by as much as 16 %, relative to the heat-addition-only case. Section 3.2 presented the argument that the heat addition process will typically dominate the type of gas dynamical situation found in scramjet combustors, and frictional, area change, and mass addition effects can be made relatively small. Using the numerical solution developed in section 3.1, the combustion influence coefficients can be calculated as in ref. [1].

A number of potentially important effects were neglected, specifically changing gas properties, i.e. molecular weight and specific heat. Inclusion of these effects would further expand the range of applicability of this analysis, but at the cost of increased numerical complexity. In fact, closed form solutions to the governing partial differential equations cannot usually be found for more than one independent variable.

Lastly, a discussion of the external nozzle process was presented. Data presented in this section showed that the assumption of an equilibrium process in the nozzle expansion is probably a reasonable assumption provided that hydrogen is the fuel

of choice. Fuels with slower chemical kinetics could be strongly impacted by non-equilibrium effects in the nozzle expansion.

References

1) Chavez, F.K.; Schmidt, D.K.; " An Integrated Analytical Aeropropulsive/Aeroelastic Model for the Dynamic Analysis of Hypersonic Vehicles"; Internal Report No. ARC92-2

2) Bilimoria, K.D.; Schmidt, D.K.; " An Integrated Development of the Equations of Motion for Elastic Hypersonic Flight Vehicles "; Internal Report No. ARC92-3

3) Shapiro, A.H.; The Dynamics and Thermodynamics of Compressible Fluid Flow, Vol. I and II; The Ronald Press Co.; 1953

4) John, J.E.A.; Gas Dynamics; Allyn Bacon, 1973

5) Drell, I.L.; Belles, F.E.; "Survey of Hydrogen Combustion Properties"; NACA Report 1383; 1958

6) Waltrup, P.J.; "Liquid Fueled Supersonic Combustion Ramjets: A Research Perspective of the Past, Present, and Future"; AIAA-86-0158; AIAA 24th Aerospace Sciences Meeting, Jan. 6-9, 1986; Reno, Nevada

7) Hill, P.G.; Peterson, C.R.; Mechanics and Thermodynamics of Propulsion; Addison-Wesley Publishing Co.; 1992

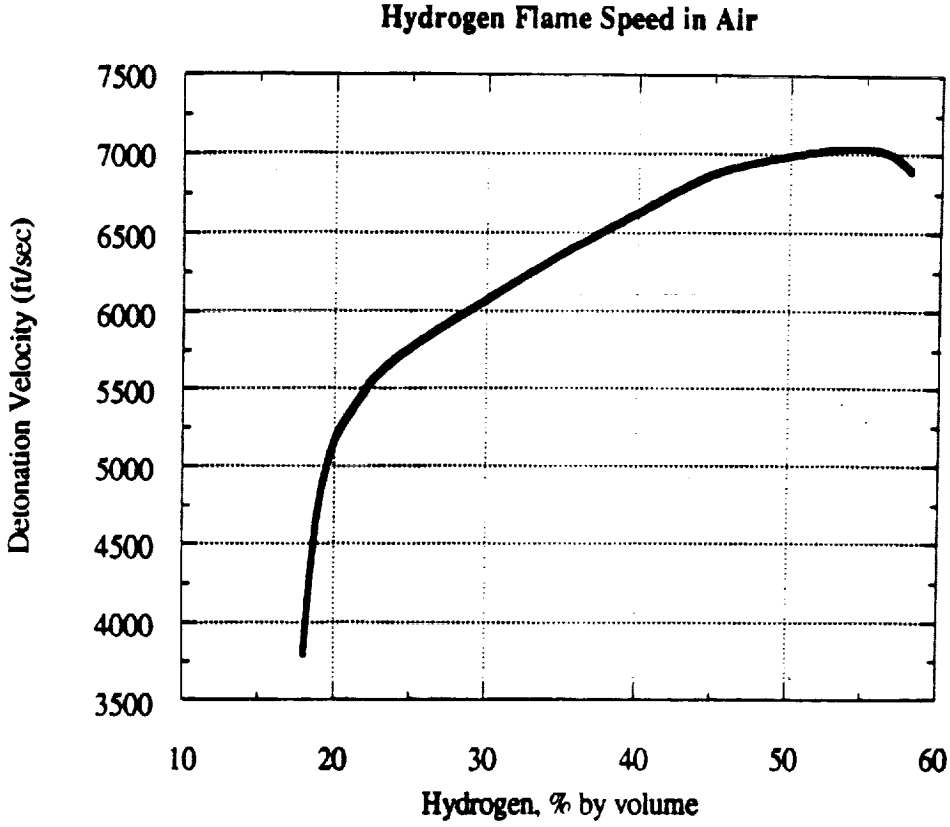

Figure 1 Hydrogen Flame Speed in air as a Function of Mixture Ratio, by Volume

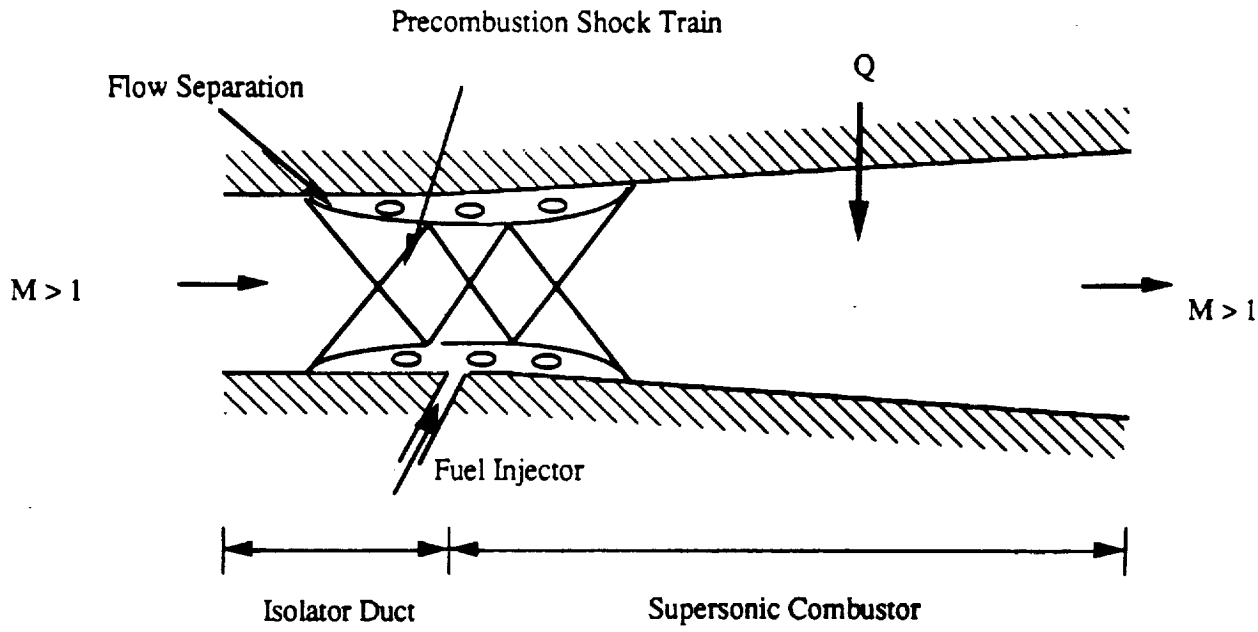

Figure 2 Isolator Duct Geometry

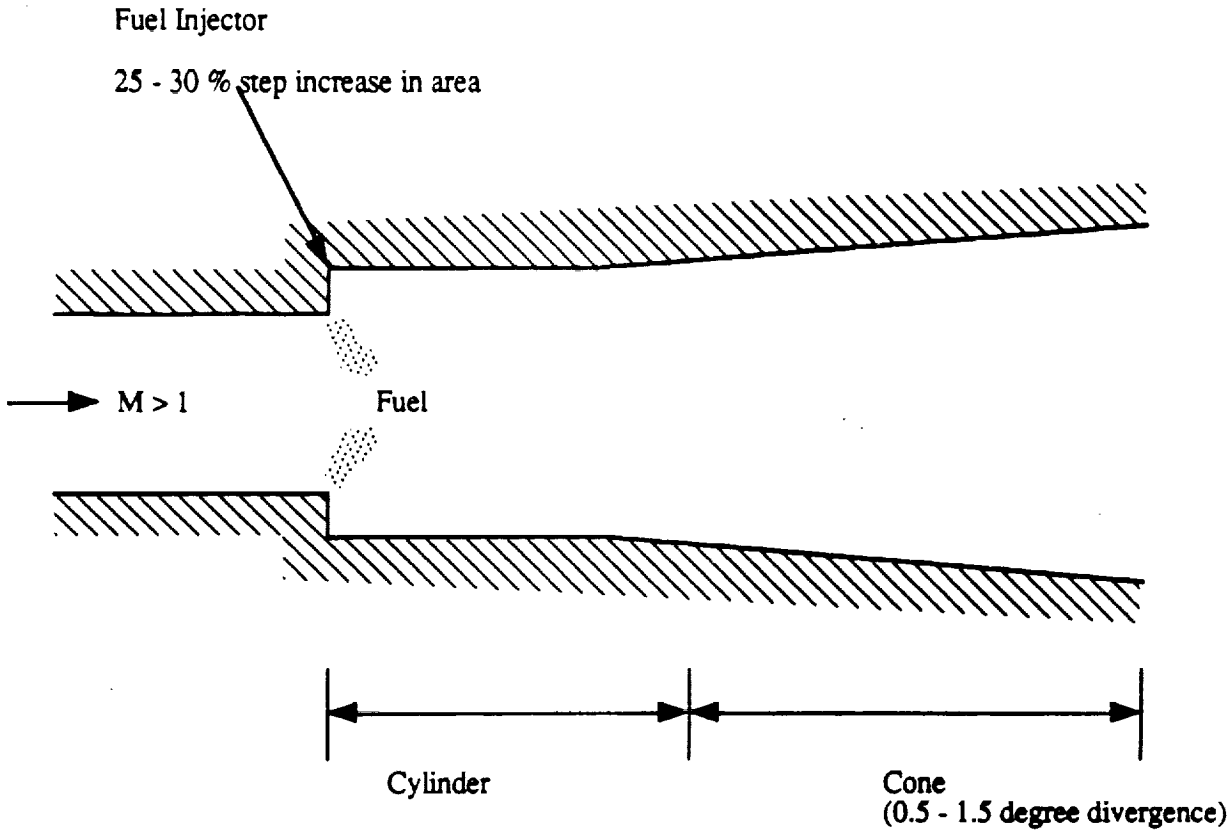

Figure 3 Supersonic Combustor Flame Holder

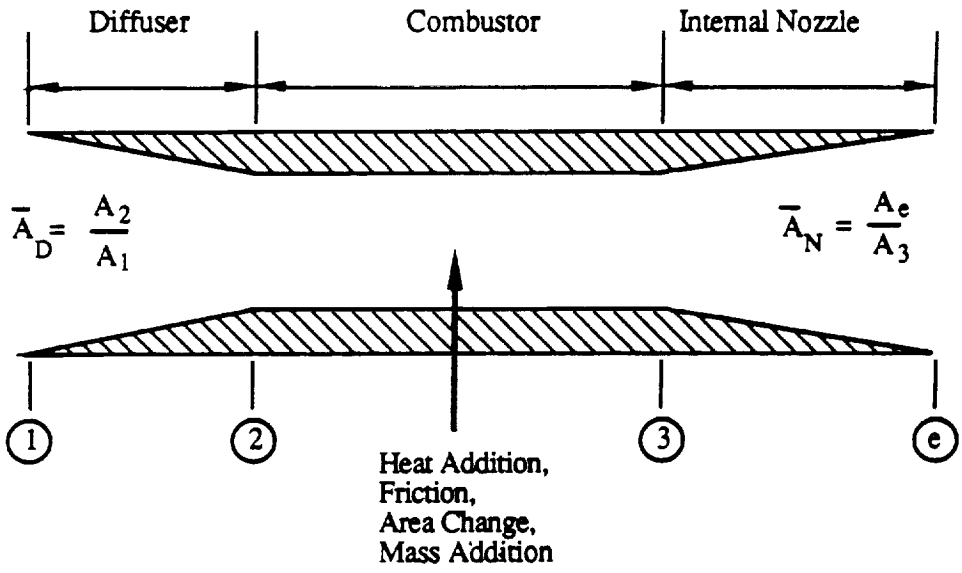

Figure 4 Scramjet Engine

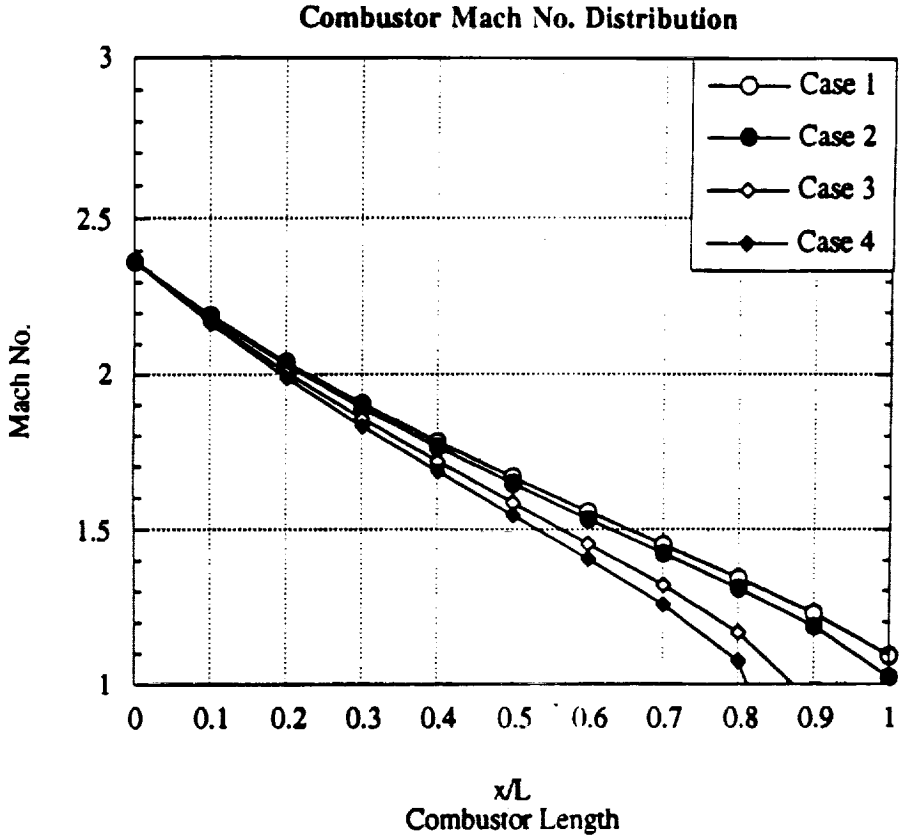

Figure 5 Combustor Mach Number Distribution

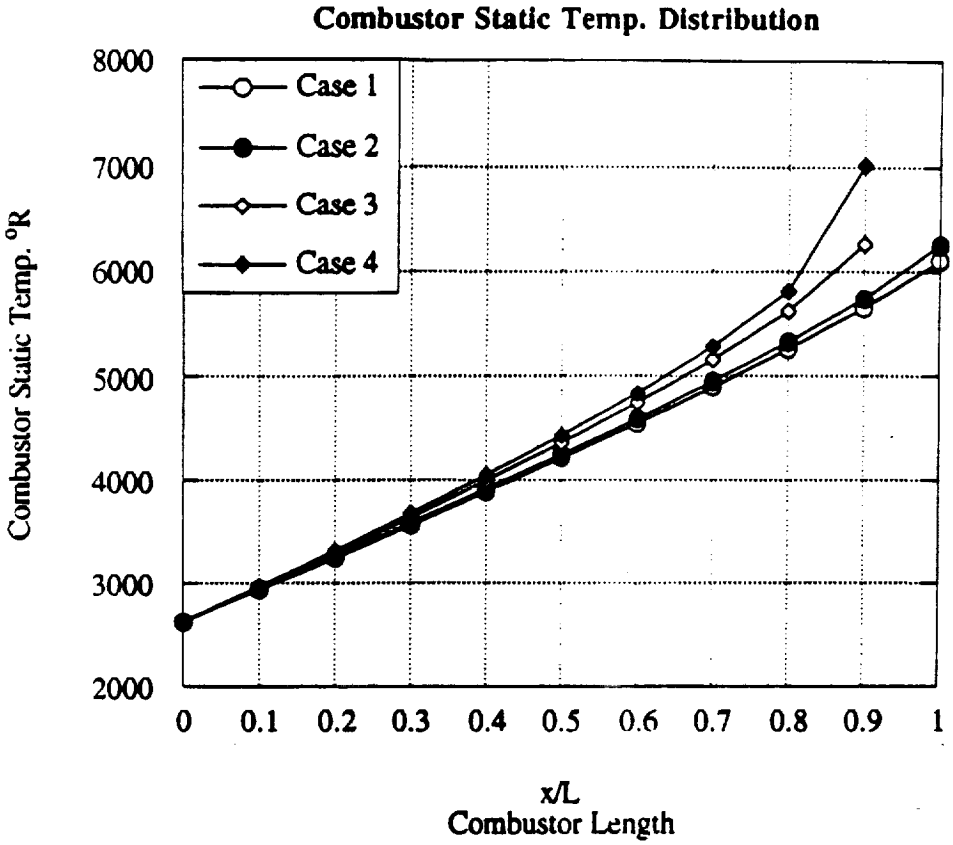

Figure 6 Combustor Static Temperature Distribution

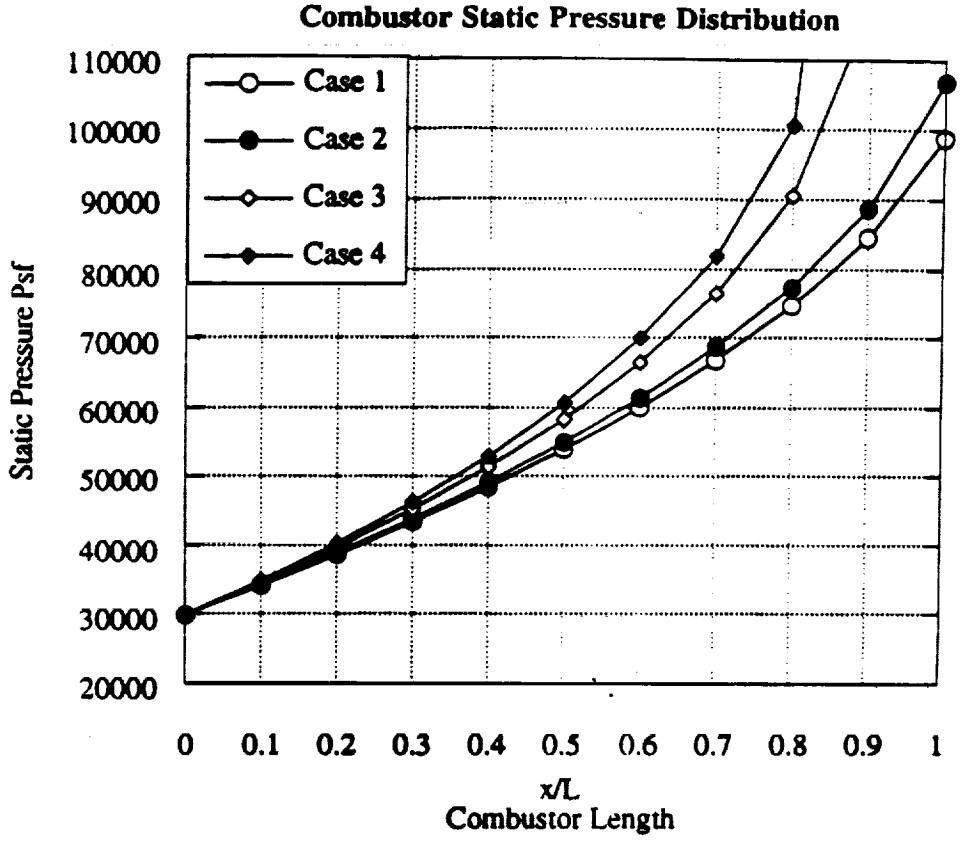

Figure 7 Combustor Static Pressure Distribution

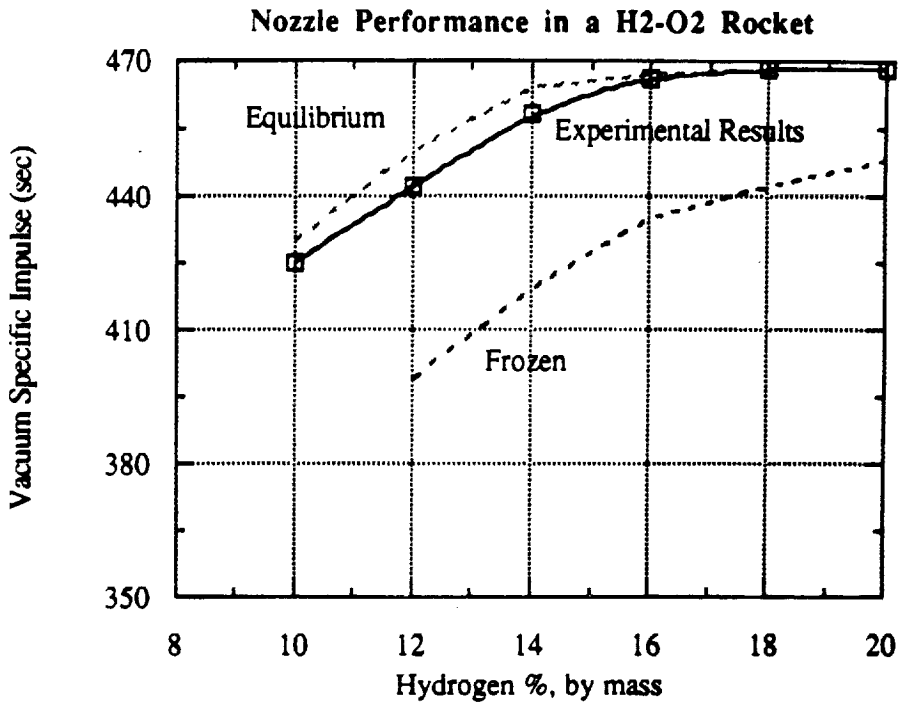

Figure 8 H2-O2 Rocket Performance Illustrating Frozen and Equilibrium Performance Limitations